2014 IEEE International Conference on Robotics & Automation (ICRA)
Hong Kong Convention and Exhibition Center
May 31 - June 7, 2014. Hong Kong, China

An In-pipe Robot with Underactuated Parallelogram Crawler Modules

Atsushi Kakogawa[1], Shugen Ma[2], and Shigeo Hirose[3]

***Abstract*— In this paper, we present a new in-pipe robot with independent underactuated parallelogram crawler modules, which can automatically overcome inner obstacles in the pipes. The parallelogram crawler modules are adopted to maintain the anterior-posterior symmetry of forward and backward movements, and a simple differential mechanism based on a pair of spur gears is installed to provide underactuated mechanisms. A central base unit connects each crawler module through foldable pantograph mechanisms. To verify the basic behavior of this robot, primary experiments in pipes with different diameters and at partial steps were conducted.**

I. INTRODUCTION

Most towns and cities depend on pipelines and their extension to further transport energy resources. While a long time has passed since people began using pipelines, their inspections became a high priority for maintaining the infrastructures, because careful and extensive work is required to check every point in a very broad area. To overcome this time-consuming task, robotic pipeline inspections have been proposed, and various types of in-pipe robots have been developed. Among them, the wheel-type is mostly used for traveling through the pipes thanks to its speed and adaptability to circumstances.

Among the wheel-type in-pipe robots, we have focused on the screw drive mechanism and its functionalities in bent and T-branched pipes because this model has the advantage of downsizing [1] [2]. For example, the screw drive mechanism requires only rotational motion with one degree of freedom and the rotational axis of the rotator coincides with the center axis of the pipe. Therefore, no driving systems, such as a pair of bevel gears, are required to change the rotational direction of the actuator. Our proposed screw drive in-pipe robot with a pathway selection mechanism can negotiate both bent pipes and T-branches with only a driving actuator and a single steering actuator [2].

On the other hand, in-pipe robots with three independent driving modules have been reported to be reliable robots for the past few years [3] [4] [5] [6]. They have several differences compared to the screw drive mechanism. Firstly, when passing through T-branches, the screw drive in-pipe robot needs an additional active joint for bending its body. In contrast, the in-pipe robot with three driving modules can steer in the T-branches by only adjusting the speed of each module, just like the counter rotation of the construction machines and tanks. These two steering methods are classified into two types: an articulated active joint and a differential-drive type, respectively [3] [4]. Although both methods are valid for forward travel, they behave differently in case of backward motion because the screw drive type has an anterior-posterior asymmetry. Even though the front rotator of the screw drive in-pipe robot can enter in the next desired pathway in the T-branch and pull the rear stator unit, it cannot push the rear unit during backward travel due to the lack of contact between the rotator and the inner surface of the T-branch (Fig. 1). The in-pipe robot with three driving modules, however, has the same performance even when traveling backward because of the anterior-posterior symmetry.

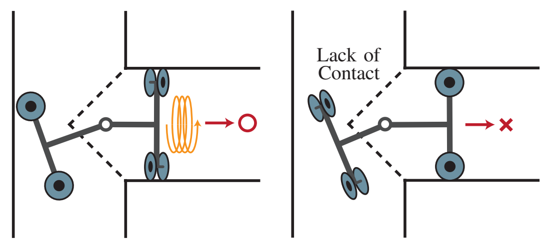

(a) Forward Movement (b) Backward Movement

Fig. 1. Forward/backward mobility of a screw drive mechanism

Moreover, the wheels of the in-pipe robot with three driving modules are suitable for both straight and bent pipes, while the front wheels of the screw drive type sweep across the pipes and they are evenly in contact with the inner surface. Thus, the path trajectory of the wheels becomes longer even if the linear travel distance of the robot is short. Consequently, the contact with inner obstacles (contamination and corrosion) increases. From the above consideration, we know that the screw drive type is effective only for smaller and relatively cleaner pipeline systems without any branch.

The inspections using the three independent driving modules might be feasible for severe conditions including contamination, bent pipes, branch pipes, and diameter change; however, the strategy to overcome these challenges has not been perfectly completed yet. For example, most of the three driving modules are passively pushed by pantographs and springs to maintain contact with the inner wall of the pipe. When the robot encounters obstacles and steps of the joints between pipes, it requires a large amount power to contract the diameter, i.e., to overcome the expanding force of the springs. To extend the range of the adaptive diameter,

[1]A. Kakogawa is with Department of Robotics, Ritsumeikan University, Eastwing Building, 1-1-1 Noji Higashi, Kusatsu, Shiga, Japan.
[2]S. Ma is with Department of Robotics, Ritsumeikan University, Eastwing Building, 1-1-1 Noji Higashi, Kusatsu, Shiga, Japan. He is also with School of Electrical Engineering & Automation, Tianjin University, China. shugen@se.ritsumei.ac.jp
[3]S. Hirose is with HiBot Corp., 2-18-3, Shimomeguro, Meguro-ku, Tokyo, Japan. hirose@hibot.co.jp

additional active arms have been proposed [6]. Moreover, the speed of each driving module should be properly controlled when traveling through bent pipes. Therefore, a control method based on geometric and kinematic analysis has been adopted [3] [5]. In a previous study, a clutch-based selective drive mechanism that can switch active and passive wheels on each module has been proposed [4]. In addition, a method using angle sensors to detect the attitude of each module has been introduced [6]. This robot can pass through bent pipes by keeping the attitude of each module constant; thus, it requires no geometric and kinematic analysis.

However, the increase in the number of actuators and sensors leads to an increase in the size, weight, and operation difficulty of the robot. Therefore, we propose a new in-pipe robot with three underactuated parallelogram crawler modules (Fig. 2). Table I shows the specifications of the proposed robot. It can automatically adapt to the diameter change and inner obstacles without any additional active arms. Here, we describe the design of the new robot and present the primary experimental result that the robot passed through a stepped straight pipe.

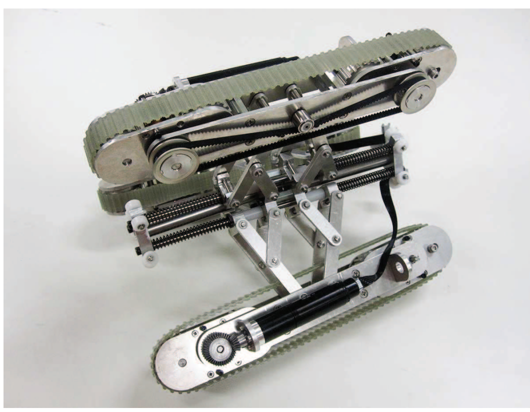

Fig. 2. A mechanical model of the developed in-pipe robot with underactuated parallelogram crawler modules

TABLE I
SPECIFICATIONS OF THE ROBOT

Adaptive Diameter [mm]	$\phi136$ - $\phi226$
Axial Length [mm]	235
Total Weight [kg]	1.8
Maximum Speed [m/s]	0.23
Rated Torque of the Geared Motor [Nm]	0.332

II. MECHANISM

The newly developed in-pipe robot consists of three underactuated parallelogram crawler modules that are radially connected with an interval of 120°. Each underactuated parallelogram crawler module consists of an underactuated parallelogram mechanism and a foldable mechanism. We used the parallelogram for two reasons. First, the length of the belt is constant even when the crawler's shape is transforming; thus, the robot requires no additional mechanism to adjust the belt length. Secondly, the anterior-posterior symmetric transformation can be easily realized as depicted in Fig. 3. Consequently, a functionality similar to forward movement can be achieved while retrieving the robot. This function is useful for in-pipe robots that cannot turn $180°$.

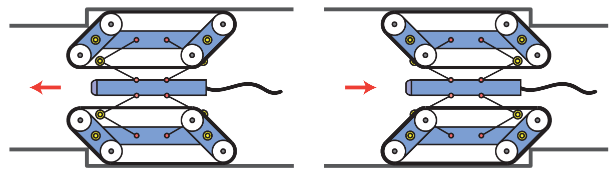

(a) Forward Movement (b) Backward Movement

Fig. 3. Similar mobility for anterior-posterior symmetric transformation

Fig. 4 shows the cross-sectional view of the CAD model of an underactuated parallelogram crawle. A single-geared motor is mounted outside of the crawler module because of the limited space. The input torque from the motor gives two outputs through the bevel gears and a differential mechanism located at the front arm. The front and rear arms are bound by a timing belt and the two rotational axes are connected by an additional narrow belt for their synchronization. Each function of these differential and synchronization belt is explained below.

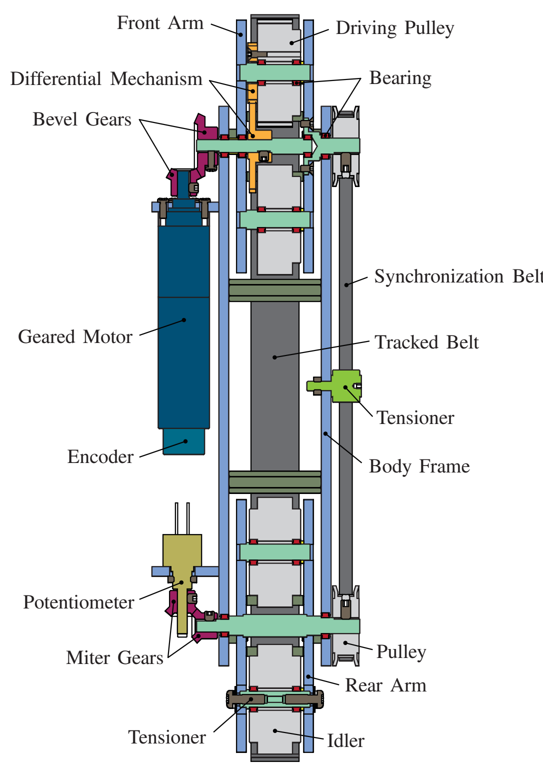

Fig. 4. A CAD model of an underactuated parallelogram crawler module

A. A Pair of Spur Gears Realize the Differential Motion

Generally, underactuated crawler robots need a differential mechanism and reducers with high gear reduction ratio, such as planetary gear reducers, for lifting the arms and the entire body [7] [8]. However, they cannot be equipped in in-pipe robots because of the limited size of the pipes. A simple differential mechanism with only a pair of spur gears was introduced to solve this problem [9]. As shown in Fig. 5 (a), the input force from the motor is transmitted to the front pulley via a set of spur gears for normal driving mode. During this mode, the front and rear arms are laid down because of the gravity and the spring force of the pantograph, thus preventing the rotation of the arms. In an open field, the crawler with undeformable polygonal shape has been often used for its high mobility; however, it is not suitable for a pipe with limited space because of its height. Our transformable crawler returns to a flat shape by itself by shortening its contractive diameter.

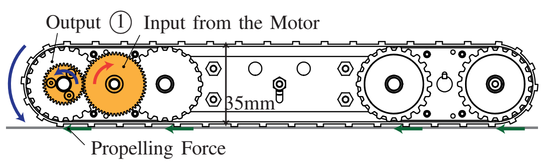

(a) Driving mode

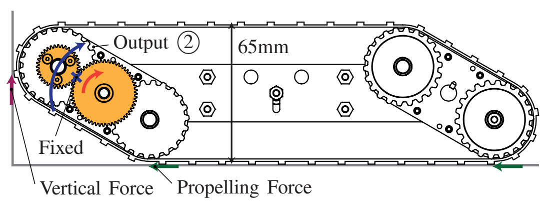

(b) Parallelogram mode (arm-lifting)

Fig. 5. The two modes of the differential mechanism

Furthermore, in the parallelogram mode presented in Fig. 5 (b), the forward motion is constrained; consequently, the input gear starts to lift the arm to 65 mm and compress the pantograph. Simultaneously, a vertical force as indicated in Fig. 5 (b) also acts on the contact point between the forepart and obstacles. This is the most important characteristic for selecting a differential mechanism. In other words, gears for the high reduction ratio can be avoided if rotational direction of the arm generated by the vertical propelling force of the pulley coincides with that of the arm axis (second output).

In Fig. 6, the teeth numbers of the bevel gears and spur gears are denoted as i_1, i_2, i_3, and i_4, respectively.

Each gear ratio is set as $i_1 : i_2 = 1 : 2$, $i_3 : i_4 = 1.6 : 1$. Generally, the output ratio for the arm-lifting should be much higher than that for normal driving. In the parallelogram mode, the motor power is transmitted to rotate the whole arm without reduction. Therefore, the speed of the front pulley is increased using a smaller gear than that of the arm axis. Torque driving the front pulley $\tau_{\rm p}$ and that of the arm $\tau_{\rm a}$ can

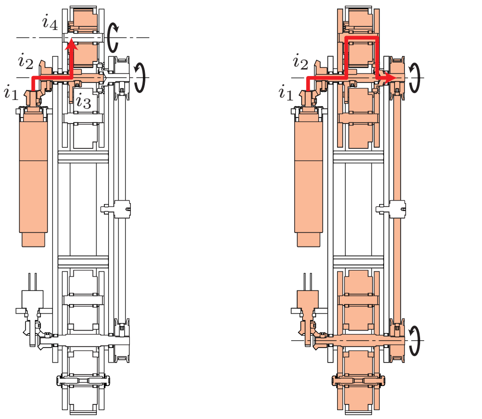

(a) First output for driving (b) Second output for arm-lifting

Fig. 6. Power transmission flow

be thus calculated by

$$\tau_{\rm p} = \frac{i_4 i_2}{i_3 i_1}\tau_{\rm m} \quad (1)$$

$$\tau_{\rm a} = \frac{i_2}{i_1}\tau_{\rm m}, \quad (2)$$

where $\tau_{\rm m}$ is the rated torque of the geared motor. Finally, $\tau_{\rm p} = 0.415$ Nm and $\tau_{\rm a} = 0.664$ Nm are derived.

Moreover, this underactuated crawler can absorb impacts from the unexpected external forces but not from breaking down the motors [7]. It also has the ability to absorb the internal force generated between misaligned crawler modules.

B. Synchronization between Front Arm and Rear Arm

The belt might be loose if the front and rear arms are not linked because the perimeter traced by the four pulleys is shorter than that of the belt. This problem can be avoided by a parallel link mechanism. However, the arms need to be raised from the singular point and, therefore, the shape of the crawler may not become a parallelogram [10]. To avoid this dead point, a timing belt is utilized to directly rotate both axes of the front and rear arms as depicted in Fig. 6 (b). The angle of the lifting arm can be detected by a potentiometer mounted on the axis of the rear arm.

Moreover, in the parallelogram mode, if the front pulley is constantly locked by the friction, the arms continuously rotate to the backward direction. To prevent this, stopper pins are fixed to prevent the arms from lifting more than $30°$ (Fig. 7). After the rotational angle of the arm reaches $30°$, the crawler starts to drive with transformation.

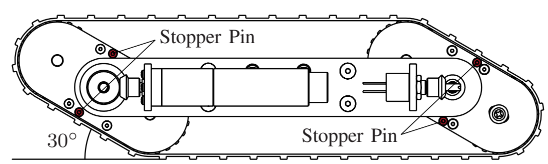

Fig. 7. Stopper pins used to limit the arm rotational angle of the arm

C. Foldable Mechanism

To change the adaptive diameter, each crawler module is connected to a central base unit through passive pantograph mechanisms (Fig. 8). Each pantograph is radially assembled with an interval of 120°. A slider moves along the horizontal shaft that is passively pushed by a 0.3 N/mm spring. As previously mentioned, the spring force and gravity push the arm down while in driving mode. The end of the link is set at the middle part of the crawler (Joint A and B) because there is no space elsewhere due to the presence of the front and rear arms. Due to their geometric nature, Joints A and B can only move vertically. Hence in theory, the crawler module cannot have a relative angle to the central base unit because the distance between Joint A and B is constant.

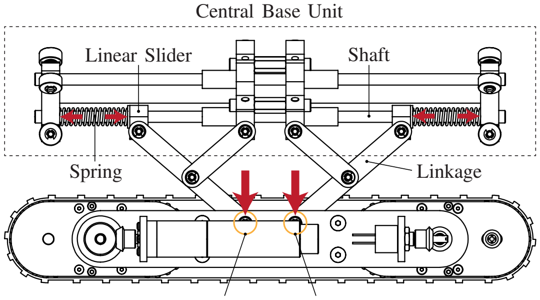

Fig. 8. A pantograph mechanism used to change the diameter of the robot

However, as depicted in Fig. 9 the positions of these two joints can move independently because each linkage has a certain axial interspace [3]. Without this effect, the crawler is kept parallel to the pipe even when transforming, which is not feasible for adaptive movement.

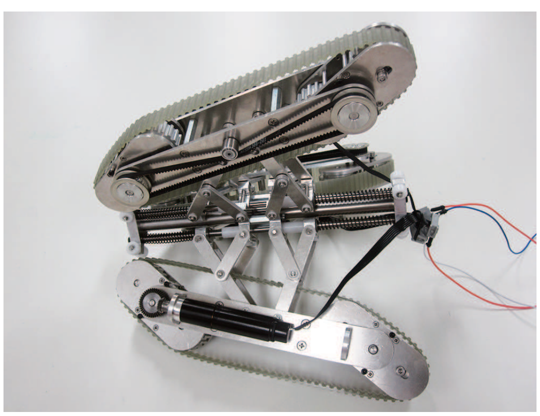

Fig. 9. Uneven posture eventually generated

When the pantograph is compressed to the limit, the transforming tracked belt might touch the central base unit. Here, to smoothly drive the belt, free guide rollers are attached (Fig. 10).

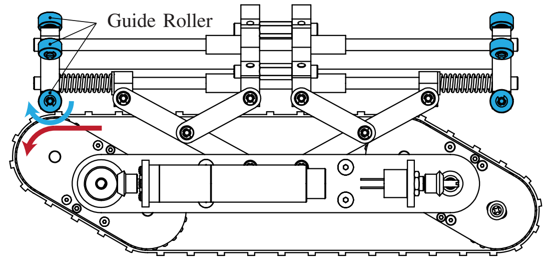

Fig. 10. Guide roller to guarantee smooth motion of the belt

D. Adaptive Diameter of Pipes

Diameter of the proposed in-pipe robot depends on two factors: contractile range of the foldable mechanism and height of the parallelogram crawler modules. When the crawler module does not transform its shape (normal driving mode), and the foldable mechanism is most contracted, the adaptive diameter of the robot becomes minimum (Fig. 11 (a)). In contrast, when the foldable mechanism is most expanded by the spring, the robot cannot enlarge its diameter any more (Fig. 11 (b)). The contractile range of the foldable mechanism is dependent on the length of the linkage and solid length of the spring. From this state, the diameter of the robot can be further extended through the use of the shape-transforming function of the parallelogram crawler (Fig. 11 (d)). Lower crawler modules can touch the inner wall of the pipe due to the gravity and generate the propulsive force in horizontal pipes even if the diameter of the pipe is larger than that of the robot. However, this function becomes effective in vertical pipes where the conventional in-pipe robots cannot reach the inner wall of the pipe. Fig. 11 (c) shows the limitation that the parallelogram crawler can completely transform its shape. This height of parallelogram crawler module is dependent on length of the front arm and position of the stopper pins.

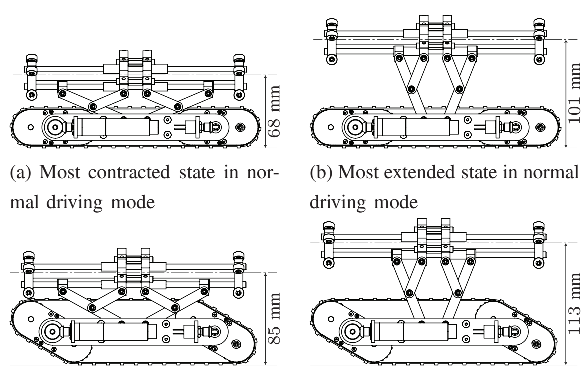

(a) Most contracted state in normal driving mode

(b) Most extended state in normal driving mode

(c) Most contracted state in parallelogram mode

(d) Most extended state in parallelogram mode

Fig. 11. Adaptive Diameter of Pipes

III. EXPERIMENTAL TEST

To verify the fundamental capability of the new in-pipe robot with underactuated parallelogram crawler modules, two experiments were conducted. In both cases, a constant supply of 12 V is provided to the three motors in parallel.

A. Experimental Test in a Connected Pipes with Large Diameter Change

Fig. 12 shows the first experimental setup used to test the mobility of the robot when the pipes undergo large diameter changes. Two vinyl chloride pipes of $\phi 202$ mm (transparent) and $\phi 154$ mm in diameter are joined by a circular truncated cone-like pipe called an increaser. This increaser is standardized as "AS-12" by Japan PVC Pipe and Fittings Association. The diameter difference is about 48 mm, thus, each crawler module needs to be contracted by 24 mm. The distance and height of the constricted part are 50 mm and 28 mm, respectively. Thus, the gradient angle is approximately 30°. The robot is inserted from the side of the larger pipe ($\phi 202$ mm).

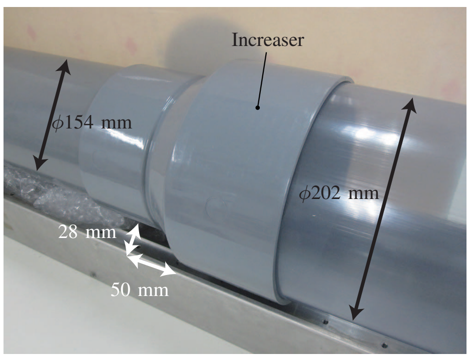

Fig. 12. Experimental setup of different pipes

The sequences shown in Fig. 13 show that our proposed in-pipe robot negotiates the constricted pipe. Initially, all arms are pressed to the inner wall of the pipe. When the crawler collides against the diameter change in sequence 2, it begins to transform. In sequence 3, the transformation amount of the lower crawler module is small because the two upper crawler modules overlie it. From sequence 4 to 6, the robot takes an uneven posture similar to that of Fig. 9, and then it goes into the smaller pipe.

B. Experimental Test in a Pipe with a Partial Step

For the second experiment, a straight pipe with an inner rubber step was prepared as shown in Fig. 14. It corresponds to the condition that the inner surface of the pipe is partially deformed or contaminated, because the friction between the tracked belt and the rubber sheet is approximately 0.8, which is twice as much as that between the belt and the inner wall of the vinyl chloride pipe. The maximum height of this step is 35 mm.

Fig. 15 shows the experimental sequences in a straight pipe with a partial step. While the robot is climbing a step, the lower crawler module does not transform but the two upper arms are lifted up. This is because if any one of the three modules motion is prevented, the others are also restricted by the linked central base. As a result, the motor's

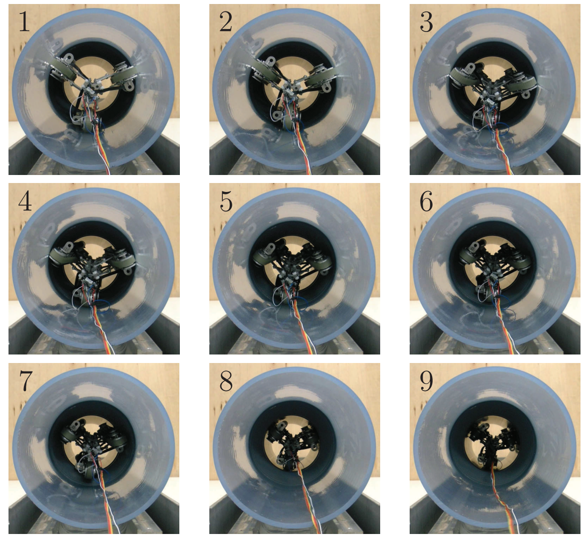

Fig. 13. Experimental sequence of diameter change

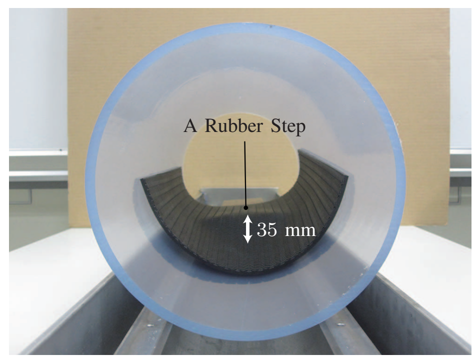

Fig. 14. Experimental setup for a partial step

power is transmitted to the arm-lifting action. Therefore, transformation is feasible even if the friction does not act on to the crawler.

C. Comparison with the In-pipe Robot without Parallelogram Mode

To compare the mobilities between the robots with parallelogram mode and without it, an additional experiment is conducted by adding a hook to restrict the arm-lifting motion as shown in Fig. 16.

The experiment showed that each crawler module can reach the next smaller pipe by the aforementioned effect in Fig. 9. However, it cannot move forward any more from this state because the side parts of the crawler modules (motor and synchronization belt) contact with the edge of the step. We know from this result that shape-transforming of the parallelogram crawler enhances the mobility in a stepped pipe. However, this problem may be also solved by only using thick grouser. This point should be discussed by combining with the contractile range of the foldable mechanism in the future. If the height of the crawler gets largers, the adaptive diameter of the in-pipe robot becomes

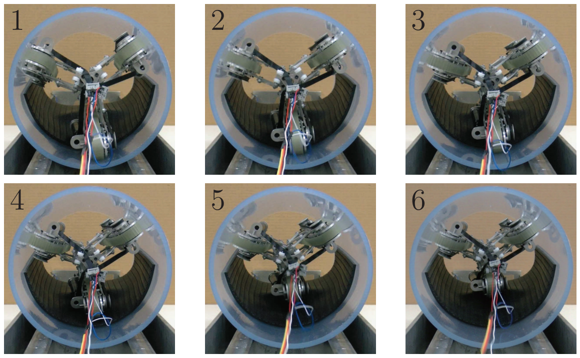

Fig. 15. Experimental sequence in a straight pipe with a partial step

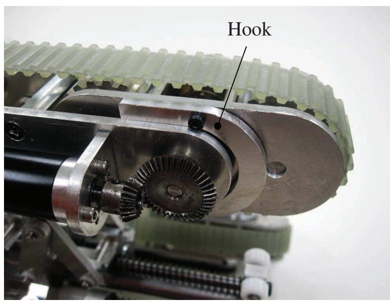

Fig. 16. Hook to restrict the arm-lifting motion

smaller.

IV. CONCLUSIONS AND FUTURE WORKS

Here, we have presented a newly developed in-pipe robot with underactuated parallelogram crawlers along with the validation of its features. The main features of the developed in-pipe robot are as follows:

- Needlessness of the belt-perimeter adjusting mechanism
- Anterior-posterior symmetric transformation of the parallelogram
- Differential mechanism providing two outputs for driving and climbing movement through a single actuator
- Expansion of the contractible diameter range by switching the parallelogram and flat crawlers
- Impact absorption of the underactuated mechanism

However, this is only the first stage of the project and additional work is required in the future. First, the feedback control has not been discussed yet. To make the robot pass through bent and branch pipes, speed control should be conducted.

Furthermore, identical power is distributed to the three motors, sometimes causing misalignment (Fig. 17), especially after overcoming obstacles. One of the reasons is the gravity, because the lower modules support the upper modules. As a result, the position of the central base unit lowers. This phenomenon can be solved by controlling each module separately. By taking advantage of the different speeds among the three modules, the posture of the body can be aligned.

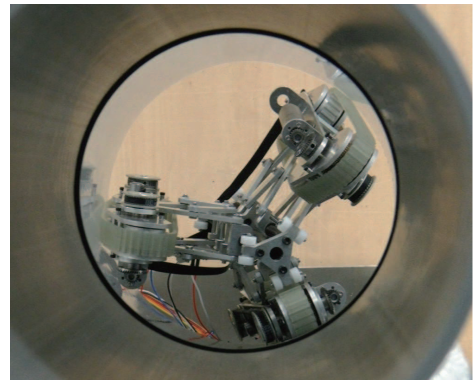

Fig. 17. Misaligned crawler modules

In addition, wire management and waterproofing should be considered to achieve a more practical use. In-pipe robots need to be tethered to supply power and signals, because battery and wireless communication are not reliable in underground pipes or iron pipes. However, wire might hook the corner of the bent and branch pipes. To solve this problem, whole stem drive [11] or additional driving units should be adopted. Also, current design of the parallelogram crawler is not waterproofed. Both side of the parallelogram crawler module (motor, potentiometer, and synchronization belt) should be covered to protect from water and dust.

REFERENCES

[1] A. Kakogawa and S. Ma, Stiffness Design of Springs for a Screw Drive In-pipe Robot to Pass through Curved Pipes and Vertical Straight Pipes, Int. J. Advanced Robotics, vol. 26, no. 3/4, 2012, pp. 253-276.

[2] T. Nishimura, A. Kakogawa and S. Ma, Pathway Selection Mechanism of a Screw Drive In-Pipe Robot in T-Branches, in Proc. IEEE Int. Conf. Automation Science and Engineering, Seoul, Korea, 2012, pp. 612-617.

[3] S. Roh and H. R. Choi, Differential-drive In-pipe Robot for Moving inside Urban Gas Pipelines, IEEE Trans. Robotics, vol. 21, no. 1, 2005, pp 1-17.

[4] S. Roh, D. W. Kim, J. Lee, H. Moon, and H. R. Choi. In-pipe Robot Based on Selective Drive Mechanism, Int. J. Control, Automation, and Systems, vol. 7, no. 1, 2009, pp. 105-112.

[5] Y. S. Kwon and B. J. Yi, Design and Motion Planning of a Two-Module Collaborative Indoor Pipeline Inspection Robot, IEEE Trans. Robotics, vol. 28, no. 3, 2012, pp 681-696.

[6] J. Park, D. Hyun, W. H. Cho, T. H. Kim, and H. S. Yang, Normal-Force Control for an In-Pipe Robot According to the Inclination of Pipelines, IEEE Trans. Industrial Electronics, vol. 58, no. 12, 2011, pp 5304-5310.

[7] Q. Quan and S. Ma, Development of a Modular Crawler for Tracked Robots, Int. J. Advanced Robotics, vol. 25, no. 13/14, 2011, pp 1839-1849.

[8] B. Kim, Q. Vu, J. Song, and C. Yim, Novel Design of a Small Field Robot with Multi-active Crawlers Capable of Autonomous Stair Climbing, J. Mechanical Science and Technology, vol. 24, no. 1, 2010, pp 343-350.

[9] Z. Li, S. Ma, B. Li, M. Wang, and Y. Wang, Design and Basic Experiments of a Transformable Wheel-Track Robot with Self-adaptive Mobile Mechanism, in Proc. IEEE Int. Conf. Intelligent Robots and Systems, Taipei, Taiwan, 2010, pp. 1334-1339.

[10] C. Ye, G. Lv, S. Ma, and H. Ni, Development of a Variable Parallelogram Tracked Mobile Robot, in Proc. IEEE Int. Conf. Robotics and Biomimetics, Guangzhou, China, 2012, pp. 2156-2160.

[11] S. Hirose, H. Ohno, T. Mitsui, and K. Suyama, Design of In-pipe Inspection Vehicles for $\phi 25$, $\phi 50$, $\phi 150$ Pipes, in Proc. IEEE Int. Conf. Robotics and Automation, Detroit, Michigan, 1999, pp. 2309-2314.